

## RESEARCH ARTICLE

# A cytosolic reductase pathway is required for efficient N-glycosylation of an STT3B-dependent acceptor site

Marcel van Lith<sup>1</sup>, Marie Anne Pringle<sup>1</sup>, Bethany Fleming<sup>1</sup>, Giorgia Gaeta<sup>1,3</sup>, Jisu Im<sup>1,2</sup>, Reid Gilmore<sup>4</sup> and Neil J. Bulleid<sup>1,\*</sup>

## ABSTRACT

N-linked glycosylation of proteins entering the secretory pathway is an essential modification required for protein stability and function. Previously, it has been shown that there is a temporal relationship between protein folding and glycosylation, which influences the occupancy of specific glycosylation sites. Here, we used an *in vitro* translation system that reproduces the initial stages of secretory protein translocation, folding and glycosylation under defined redox conditions. We found that the efficiency of glycosylation of hemopexin was dependent upon a robust NADPH-dependent cytosolic reductive pathway, which could be mimicked by the addition of a membrane-impermeable reducing agent. We identified a hypoglycosylated acceptor site that is adjacent to a cysteine involved in a short-range disulfide. We show that efficient glycosylation at this site is influenced by the cytosolic reductive pathway acting on both STT3A- and STT3B-dependent glycosylation. Our results provide further insight into the important role of the endoplasmic reticulum redox conditions in glycosylation site occupancy and demonstrate a link between redox conditions in the cytosol and glycosylation efficiency.

**KEY WORDS:** MagT1, STT3A, STT3B, TUSC3, Disulfide formation, Glycosylation, Oligosaccharyl transferase

## INTRODUCTION

Proteins entering the secretory pathway are subject to a variety of modifications, the most prevalent of which include N-linked glycosylation and disulfide formation (Bulleid, 2012; Cherepanova et al., 2016). N-glycosylation is catalysed by one of two oligosaccharyl transferases (OSTs) that transfer a pre-formed oligosaccharide from a dolichol phosphate intermediate to asparagine residues on the polypeptide chain within the consensus sequence N-X-S/T, where X is any amino acid other than proline (Kelleher et al., 2003). The two OST isoforms are multi-subunit


complexes characterised by the catalytic subunits STT3A or STT3B. They have common subunits as well as complex-specific subunits, including DC2 (also known as OSTC) and KCP2 (also known as KRTCAP2) for the STT3A complex and the thioredoxin-domain-containing proteins MagT1 or TUSC3 for the STT3B complex (Blomen et al., 2015; Roboti and High, 2012; Shibatani et al., 2005). It has been demonstrated previously that the STT3A complex associates with the endoplasmic reticulum (ER) translocon (Braunger et al., 2018; Shibatani et al., 2005) and catalyses the co-translational glycosylation of proteins, whereas the STT3B complex glycosylates sites skipped by STT3A, acting predominantly post-translationally (Cherepanova et al., 2014; Ruiz-Canada et al., 2009). Because of their distinct specificities, some substrates require the STT3A or STT3B complexes for efficient glycosylation (Cherepanova and Gilmore, 2016; Cherepanova et al., 2014). Indeed, recent proteomic analyses of glycoproteins synthesised in either STT3A- or STT3B-depleted cells have identified classes of STT3A- and STT3B-dependent N-glycosylation sites (Cherepanova et al., 2019). Deficiency of the STT3B complex cannot be compensated by the STT3A complex, resulting in hypoglycosylation of substrates, affecting their function and leading to disease pathologies linked to immunodeficiency (Blommaert et al., 2019; Matsuda-Lennikov et al., 2019).

Utilisation of potential glycosylation sites or sequons is not guaranteed and is dependent on the position within the chain (Nilsson and von Heijne, 2000; Ruiz-Canada et al., 2009; Shrimal et al., 2013) or the amino acid context of the site (Shrimal and Gilmore, 2013), with the kinetics of the folding or collapse of the polypeptide chain affecting glycosylation. Sequons buried within a protein structure, present at the amino or carboxy terminus or close to cysteines involved in disulfide formation may be underutilised, giving rise to heterogeneity in glycoprotein forms. Hypoglycosylation of sequons due to disulfide formation can be dependent upon STT3A or STT3B and is reversed when proteins are prevented from forming disulfides under highly reducing conditions (Allen et al., 1995; Cherepanova et al., 2014). In addition, STT3B-dependent glycosylation of cysteine-proximal sites requires the oxidoreductase activity of the thioredoxin-domain-containing subunits MagT1 or TUSC3 (Cherepanova and Gilmore, 2016; Cherepanova et al., 2014). Structural analysis of TUSC3 indicates its direct binding to cysteine-containing peptides, suggesting direct binding to the polypeptide to slow down protein folding and disulfide formation, allowing glycosylation to occur (Mohorko et al., 2014). The fact that MagT1 is mainly oxidised in cells (Cherepanova et al., 2014) would suggest that it acts as a reductase, thereby preventing disulfide formation prior to glycosylation. Taken together, these observations indicate a crucial role for the STT3B complex in coupling disulfide formation and glycosylation to maximise utilisation of cysteine-proximal acceptor sites.

<sup>1</sup>Institute of Molecular, Cell and Systems Biology, College of Medical Veterinary and Life Sciences, Davidson Building, University of Glasgow, Glasgow, G12 8QQ, UK.

<sup>2</sup>Cellular Protein Chemistry, Faculty of Science, Utrecht University, 3584 CH Utrecht, The Netherlands. <sup>3</sup>Nuffield Department of Orthopaedics, Rheumatology and Musculoskeletal Sciences, Botnar Research Centre, Headington, Oxford OX3 7LD, UK. <sup>4</sup>Department of Biochemistry and Molecular Pharmacology, University of Massachusetts Medical School, Worcester, MA 01605, USA.

\*Author for correspondence (neil.bulleid@glasgow.ac.uk)

 M.v.L., 0000-0003-0225-5501; M.A.P., 0000-0002-1358-4610; B.F., 0000-0002-9774-1256; G.G., 0000-0001-7500-9091; J.I., 0000-0003-0972-3048; R.G., 0000-0002-1656-4041; N.J.B., 0000-0002-9839-5279

This is an Open Access article distributed under the terms of the Creative Commons Attribution License (<https://creativecommons.org/licenses/by/4.0>), which permits unrestricted use, distribution and reproduction in any medium provided that the original work is properly attributed.

Handling Editor: Jennifer Lippincott-Schwartz  
Received 31 August 2021; Accepted 27 October 2021

The temporal relationship between disulfide formation and glycosylation suggests that the redox status of the ER may contribute to sequon utilisation (Cherepanova et al., 2016). ER redox reactions are balanced to allow both disulfide formation and reduction, resulting in the formation of the correct disulfides within folding proteins (Bulleid and van Lith, 2014). Members of the protein disulfide isomerase (PDI) family are thioredoxin-domain-containing proteins that catalyse disulfide exchange reactions (Bulleid, 2012). Their oxidation is catalysed by Ero1 proteins, which couple the reduction of oxygen to the formation of a disulfide in PDI (Cabibbo et al., 2000). Specific members of the PDI family, such as ERp57 (also known as PDIA3) (Jessop et al., 2007) and ERdj5 (also known as DNAJC10) (Oka et al., 2013; Ushioda et al., 2008) catalyse the reduction of non-native disulfides, either allowing the correct disulfides to form or targeting misfolded proteins for degradation. Exactly how these PDI enzymes are reduced is unknown, but recent evidence suggests a role for the cytosolic reductive pathway in correct disulfide formation, driven by the reduction of thioredoxin reductase (Cao et al., 2020; Poet et al., 2017).

It is likely that the ER oxidative and reductive pathways influence the STT3B subunits MagT1 and TUSC3 during oxidoreductase activity towards cysteines proximal to sequons. Hence, the correct utilisation of sequons may well be regulated by the prevailing redox conditions within the ER. To address the role of ER redox conditions on utilisation of STT3B-dependent acceptor sites, we capitalised on a recently described *in vitro* translation system that reproduces the early stages of secretory protein ER translocation and

modification under defined redox conditions (Poet et al., 2017; Robinson and Bulleid, 2020). In this system, the redox conditions can be manipulated simply by the addition of glucose 6-phosphate (G6-P), which recycles NADPH thereby driving the cytosolic reductive pathway. When a source of ER is included during translation, the newly synthesised proteins are translocated across the ER membrane and can undergo both disulfide formation and N-linked glycosylation (Wilson et al., 1995). We chose to translate the STT3B-dependent substrate hemopexin (Cherepanova et al., 2014) in such a system, and we show that it is hypoglycosylated in the absence of added G6-P, an effect that is partially reversed upon G6-P inclusion. Our results highlight the role of ER redox in the efficiency of sequon glycosylation and reveal an unexpected role for the NADPH-dependent cytosolic reductive pathway in the function of both the STT3A- and STT3B-containing OST complexes.

## RESULTS

### A cytosolic reductive pathway determines the extent of sequon usage in an STT3B-dependent glycoprotein

Our initial experiments aimed to determine whether the redox conditions within the ER had any effect on the fidelity of sequon usage within a model protein, hemopexin, which has previously been shown to undergo hypoglycosylation when expressed in cells – a phenomenon that is exacerbated in the absence of STT3B (Shrimal and Gilmore, 2013). Hemopexin has five potential sequons and forms six disulfides (Fig. 1A). For these experiments we adjusted the redox status of our *in vitro* translation reactions by adding specific components to the rabbit reticulocyte lysate.

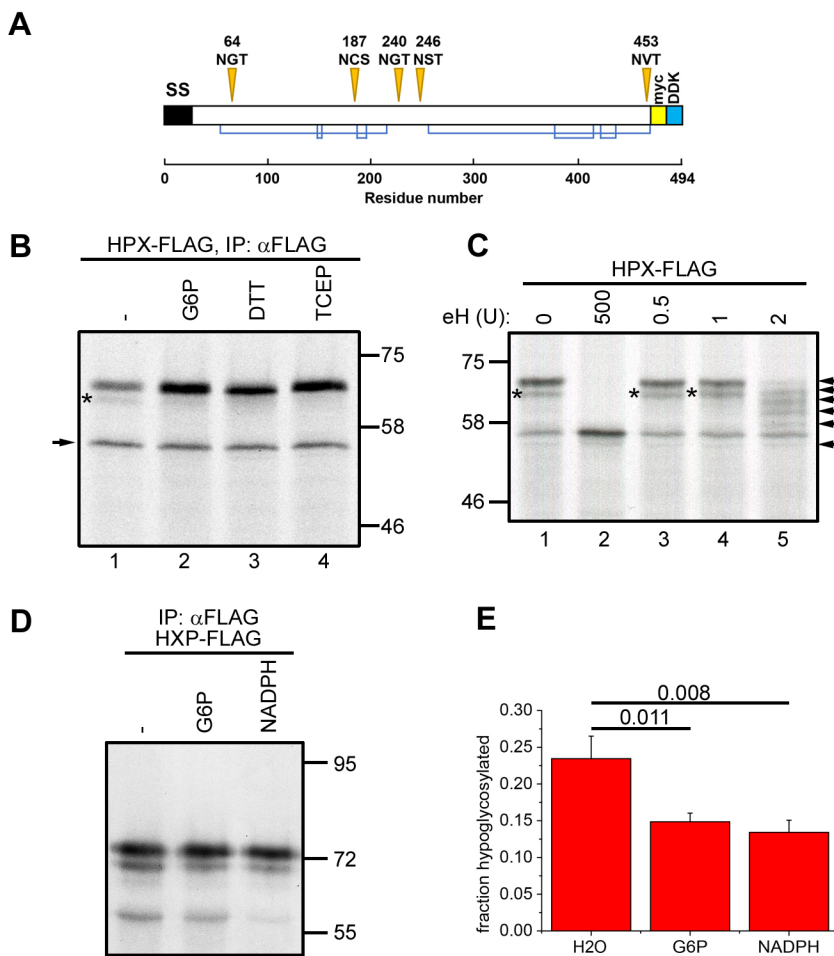


**Fig. 1. Hemopexin hypoglycosylation is prevented when G6-P or NADPH is included during translation.**

(A) Schematic diagram of hemopexin showing glycosylation sites (orange triangles) and disulfide bond connectivity (blue lines). The positions of the signal peptide (SS) and the myc- and DDK (FLAG)-tags are also indicated. (B) Hemopexin (HPX-FLAG) was translated *in vitro* in the presence of SP cells in the absence (–) or presence of 5 mM G6-P, 5 mM DTT or 1 mM TCEP for 1 h. The SP cells were washed and lysed, and hemopexin was immuno-isolated (IP) with an anti-FLAG antibody, followed by separation by SDS-PAGE. The asterisk indicates hypoglycosylated hemopexin. The arrow indicates non-translocated, non-glycosylated hemopexin. (C) Hemopexin was translated as in B in the absence of G6-P. After lysis, the samples were incubated with different amounts of endo H (indicated as units) at 37°C for 15 min and analysed by SDS-PAGE. The asterisk indicates hypoglycosylated hemopexin, and the arrows point to the different glycosylated species. (D) Hemopexin was translated as in B in the absence or presence of 5 mM G6-P or 1 mM NADPH for 30 min. The translation reactions were analysed as in B. (E) Quantification of hemopexin hypoglycosylation of three independent experiments performed as in D. Data are presented as mean  $\pm$  s.d. *P*-values from a two-tailed, two-sample unequal variance Student's *t*-tests are shown above the bar diagram. Data in B and C are representative of three and two experiments, respectively. Molecular mass markers indicated in B–D are in kDa.

We have previously shown that a commercial reticulocyte lysate that has no added dithiothreitol (DTT) allows disulfides to form in proteins synthesised even in the absence of semi-permeabilised (SP) cells as a source of ER (Poet et al., 2017). Supplementing this lysate with G6-P to drive G6-P dehydrogenase (G6PDH) and thioredoxin reductase (TrxR1) activity renders this lysate sufficiently reducing to prevent disulfide formation in proteins synthesised without SP cells but allows disulfide formation in translocated proteins when SP cells are present (Poet et al., 2017). When hemopexin was translated in the absence of added G6-P and presence of SP cells, we noted the appearance of two potential glycoforms that gave rise to a doublet after SDS-PAGE (Fig. 1B, lane 1). We also observed an additional product of ~55 kDa (Fig. 1B, arrow) that most likely corresponds to untranslocated and, therefore, unglycosylated protein. When G6-P was added to the translation, the slower migrating glycoforms predominated (lane 2). Likewise, only the slower migrating glycoform was synthesised when translations were carried out in the presence of the membrane-permeable and membrane-impermeable reducing agents DTT and tris(2-carboxyethyl)phosphine (TCEP), respectively (Fig. 1B, lanes 3 and 4). Hence it would appear that a small but significant fraction of hemopexin is hypoglycosylated in the absence of G6-P, an effect that is partially reversed when translations are carried out under more reducing conditions. As G6-P most likely alters the redox conditions by recycling NADP to NADPH in the cytosol, and because TCEP is membrane impermeable, these results suggest that the redox conditions on the cytosolic side of the ER membrane affect the glycosylation efficiency of ER-translocated hemopexin.

To verify that the two translation products seen after synthesis of hemopexin are indeed glycoproteins and to identify the status of the faster migrating band, we carried out a limited digestion of the protein with endoglycosidase (endo) H (Fig. 1C). Digestion of the translation products with the highest enzyme concentration resulted in a single band corresponding to the fully deglycosylated protein, indicating that the two products are indeed glycoforms (Fig. 1C, lanes 1 and 2). Addition of limiting amounts of endo H to the reaction allowed partial digestion, revealing all five potential glycoforms that arise from variable digestion of the five oligosaccharide side chains on hemopexin (Fig. 1C, lane 5). From this analysis, we can conclude that the two apparent glycoforms seen when hemopexin is translated in the absence of added G6-P are indeed the five- and four-glycan forms. These results are consistent with our previously observed hypoglycosylation of hemopexin when expressed in mammalian cells (Shrimal and Gilmore, 2013).

To verify that the reversal of hemopexin hypoglycosylation by G6-P is mediated by the recycling of NADP, we supplemented the translation reactions with NADPH (Fig. 1D,E). As with G6-P, we could reverse the hypoglycosylation of hemopexin just by adding NADPH, confirming that the effect is not due to G6-P directly influencing the glycosylation machinery or synthesis of the oligosaccharide side chain.

### Defining the sequon giving rise to G6-P-dependent hypoglycosylation

To determine which sequon within hemopexin is hypoglycosylated, we mutated hemopexin residues N187 and N453 to glutamine, creating single (N187Q, N453Q) and double (N187/453Q) mutants, as it has been noted previously that these sequons can frequently be skipped by the OSTs (Shrimal and Gilmore, 2013). We found that hypoglycosylation in the absence of G6-P occurred with wild-type hemopexin and hemopexin N453Q, and this could be resolved

by the addition of G6-P (Fig. 2A, lanes 1, 2, 5 and 6). Little hypoglycosylation was observed with hemopexin when N187 was mutated in either the single or double mutant (Fig. 2A, lanes 3 and 7). Quantification of the level of hypoglycosylation from three separate experiments supported the qualitative gel analysis (Fig. 2B). These results demonstrate that N187 is the acceptor site that is inefficiently glycosylated when translated in the presence of SP cells and in the absence of added G6-P.

The N187 sequon is N-C-S, with C188 forming a short-range disulfide with C200 in the native structure of hemopexin (Fig. 1A) (Paoli et al., 1999). As it has been observed previously that cysteine-proximal glycosylation sites are often skipped (Cherepanova et al., 2014), we evaluated the role of hemopexin C188 in hypoglycosylation. In addition, to determine whether the formation of the C188–C200 disulfide prevents efficient glycosylation, we mutated both cysteines individually and together to serine. We found that mutation of the more distal C200 did not prevent hypoglycosylation, which was resolved by inclusion of G6-P (Fig. 3A, lanes 5 and 6). In contrast, mutation of C188, in either the C188S single mutant or C188S/C200S double mutant, resulted in almost complete loss of hypoglycosylation (Fig. 3A, lanes 3 and 7).

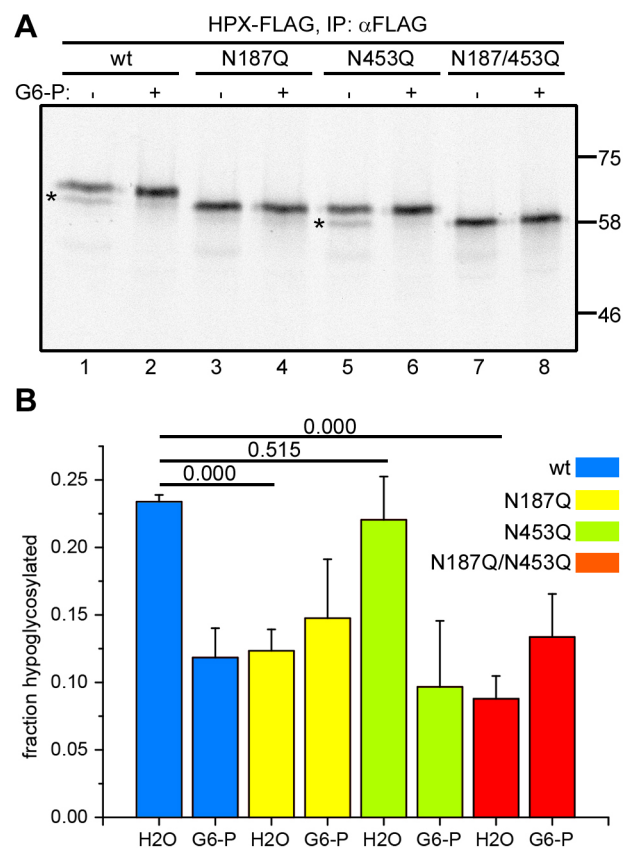


**Fig. 2. Hemopexin hypoglycosylation occurs at sequon N187.** (A) Wild-type (wt) and N-glycosylation mutants of hemopexin (HPX-FLAG) were *in vitro* translated in the presence of SP cells and in the absence (–) or presence (+) of 5 mM G6-P. The SP cells were washed and lysed, and hemopexin was immuno-isolated (IP) with an anti-FLAG antibody, followed by SDS-PAGE and autoradiography. Hypoglycosylated hemopexin is indicated by asterisks. Molecular mass markers are shown in kDa. (B) Quantification of hemopexin hypoglycosylation of three independent experiments performed as in A. Data are presented as mean ± s.d. *P*-values from Student's *t*-tests as in Fig. 1 are shown above the bar diagram. H2O, vehicle control for G6-P addition.

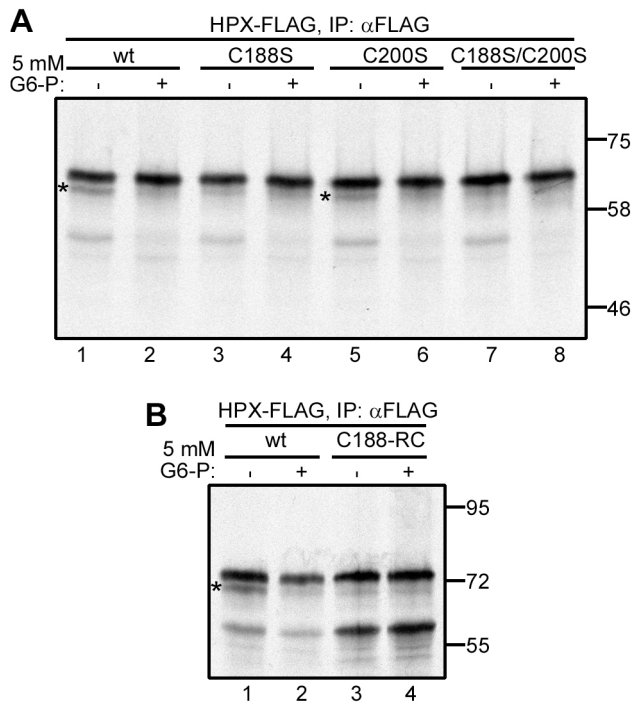


**Fig. 3. Disulfide formation via C188 results in hemopexin hypoglycosylation.** (A) Wild-type (wt) and cysteine mutants of hemopexin (HPX-FLAG) were translated *in vitro* in the presence of SP cells and in the absence (–) or presence (+) of 5 mM G6-P for 1 h. The SP cells were washed and lysed, and hemopexin was immuno-isolated (IP) and analysed by SDS-PAGE and autoradiography. Hypoglycosylated hemopexin is indicated by asterisks. (B) Wild-type hemopexin and hemopexin lacking all mature protein cysteines except C188 (C188-RC) were translated *in vitro* with SP cells in the absence or presence of 5 mM G6-P for 1 h, then analysed as in A. Hypoglycosylated hemopexin is indicated by an asterisk. Data in A and B are representative of at least three experiments. Molecular mass markers are shown in kDa.

Preventing the native disulfide from forming by mutating C200 did not stop hypoglycosylation of the acceptor site, whereas mutating C188 did, suggesting that it is the presence of the cysteine that restricts glycosylation rather than the native disulfide per se. Alternatively, C188 could be oxidised or form a non-native disulfide to an alternative cysteine to C200. To test these two possibilities, we created a construct where we mutated all the cysteines in the sequence apart from the cysteine at C188. Upon translation the protein was almost fully glycosylated, in both the presence or absence of G6-P (Fig. 3B, lanes 3 and 4). This result suggests that the formation of either a native or non-native disulfide via C188 restricts the ability of the OST to glycosylate N187, resulting in hypoglycosylation. In addition, it also shows that it is a change in the redox conditions during synthesis that is reversed by the inclusion of G6-P, maintaining C188 in a reduced state to allow efficient glycosylation.

#### Hemopexin forms distinct disulfide-bonded species during translation in the absence or presence of added G6-P

The ability of C188 to form a native or non-native disulfide affected N187 occupancy, which suggests a role for G6-P in modulating disulfide formation in our translation system. Indeed, we have previously shown that addition of G6-P prevents non-native disulfide formation in a variety of proteins by recycling NADPH and maintaining cytosolic thioredoxin in a reduced state (Poet et al., 2017). To determine the redox status of hemopexin following

translation, we prevented disulfide rearrangement following synthesis using an alkylating agent and separated the translation products under non-reducing conditions. Typically, long-range disulfides formed in proteins affect their electrophoretic mobility by altering the hydrodynamic volume of the denatured protein. When the hemopexin translation products were analysed this way, we observed several oxidised species with a greater mobility than the reduced protein (Fig. 4A, compare lanes 1 and 5). To rule out any contribution of hypoglycosylation to the pattern under non-reducing conditions, the samples were also treated with endo H to remove all glycans (Fig. 4A, even-numbered lanes). Multiple oxidised species were still observed, indicating that hemopexin forms distinct and incompletely disulfide-bonded species in our translation system.

When the translations were carried out in the presence of G6-P, most of the oxidised species migrated as those in untreated lysates (Fig. 4A, lanes 1 and 2 versus lanes 3 and 4). One species appeared after G6-P addition, seen in the endo H-treated samples (Fig. 4A, lane 2 versus lane 4, indicated by an arrow). This translation product was digested by proteinase K, indicating that it corresponds to untranslocated hemopexin (Fig. 4B, lane 4, arrow). The removal of untranslocated material was most clearly seen when the samples were separated under reducing conditions (Fig. 4B, lane 5 and 7, downward arrows). The remainder of the bands were protected from proteinase K digestion, indicating that all these species were translocated into the ER lumen. The dramatic change to the redox status of untranslocated protein is consistent with our previous studies indicating that the addition of G6-P restores a robust reducing pathway in the cytosol but does not prevent correct disulfide formation in proteins translocated across the ER membrane (Poet et al., 2017; Robinson and Bulleid, 2020). Interestingly, the oxidised species migrating with intermediate mobility became less diffuse after G6-P addition (Fig. 4A, lanes 2 and 4, vertical line and asterisk) suggesting some rearrangement of disulfides.

Adding the reductant DTT to the hemopexin *in vitro* translations prevented disulfide formation, resulting in a non-reducing pattern that resembled that of the samples run under reducing conditions (Fig. 4A, lanes 9 and 10 versus lanes 13 and 14). In contrast, addition of the membrane-impermeable reductant TCEP to the reactions gave a non-reducing pattern like that observed following G6-P addition (Fig. 4A, lanes 3 and 4 versus lanes 11 and 12), including the sharpening of the intermediate oxidised species (Fig. 4A, lane 12, asterisk). Both the addition of TCEP and G6-P altered the overall pattern of translocated disulfide-bonded forms, and TCEP (and to some extent G6-P) addition resulted in a shift in their ratios, with more of the slower migrating form present following addition (Fig. 4A, compare lanes 2, 4 and 12). Hence, G6-P inclusion caused subtle but distinct differences in the oxidised species present indicative of rearrangement of non-native disulfides. While the addition of G6-P, TCEP or DTT had different effects on the redox species formed, they all resulted in partial reversal of hemopexin hypoglycosylation.

#### G6-P does not act via an ER NADPH pool or PDIs involved in non-native disulfide reduction

The results presented so far suggest a requirement to maintain a robust cytosolic reductive pathway to ensure the efficient glycosylation of hemopexin. Alternatively, G6-P can be transported into the lumen of the ER by the glucose-6-phosphate transporter (G6PT, also known as SLC37A4), where it can be used by the ER-localised hexose-6-phosphate dehydrogenase (H6PDH, also known as H6PD) to locally generate NADPH (Clarke and Mason, 2003). The NADPH could be used to provide reducing

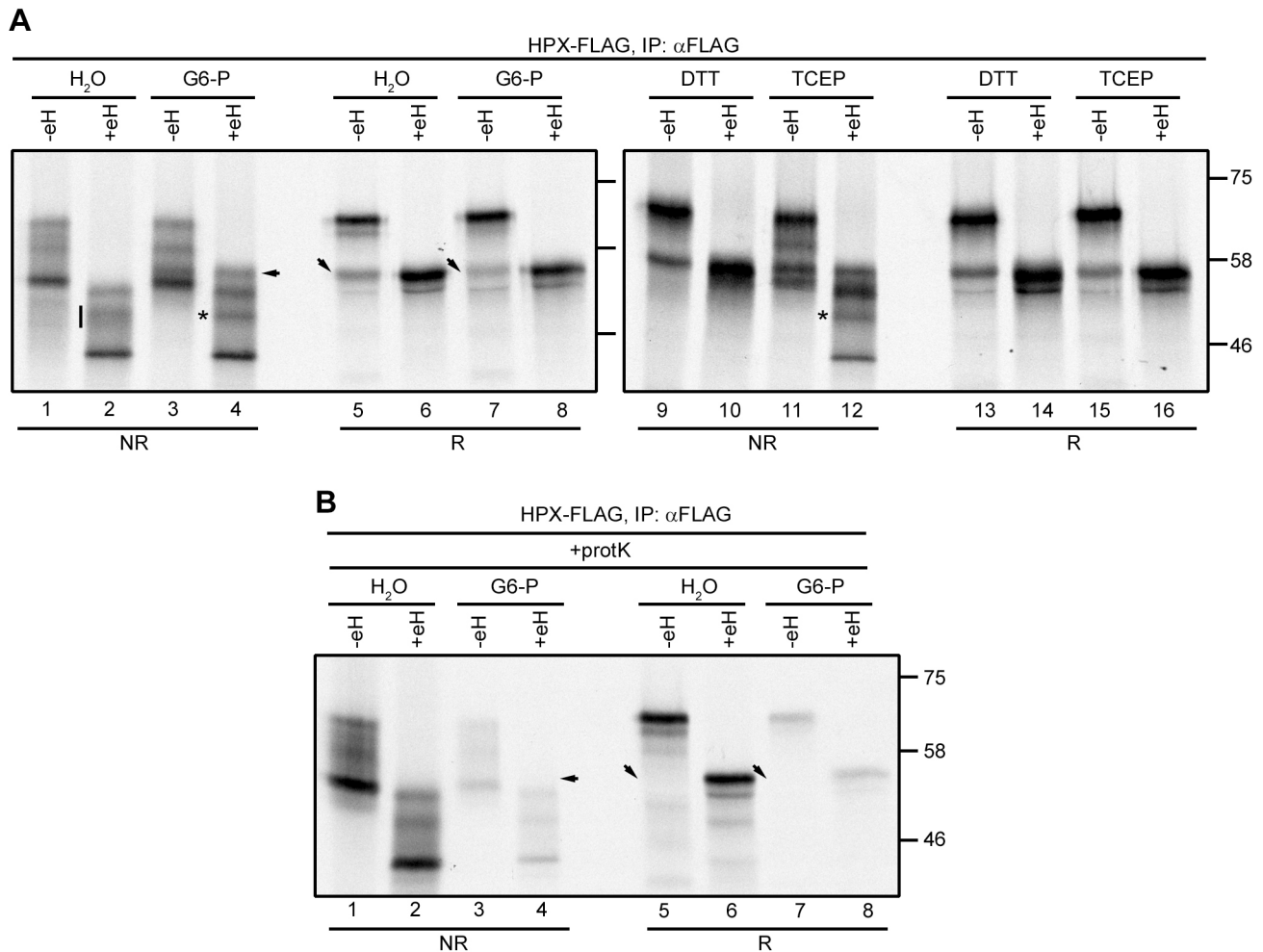


**Fig. 4. Hemopexin forms several disulfide-bonded species when translated in the presence or absence of G6-P.** (A) Hemopexin (HPX-FLAG) was translated *in vitro* in the presence of SP cells in the absence (H<sub>2</sub>O) or presence of 5 mM G6-P, 5 mM DTT or 1 mM TCEP. The translations were stopped by adding 20 mM N-ethyl maleimide (NEM) and incubation on ice. After lysis, the samples were mock treated (–eH) or treated with endo H (+eH; 500 units), followed by immuno-isolation (IP) and analysis by reducing (R) and non-reducing (NR) SDS–PAGE. The vertical line and asterisks indicate a change in oxidation state when *in vitro* translations were carried out in the presence of G6-P or TCEP. (B) Hemopexin was translated as in A. After the addition of 20 mM NEM and pelleting the SP cells, the cells were treated with proteinase K (protK), followed by lysis and endo H treatment. The samples were immuno-isolated and analysed by reducing and non-reducing SDS–PAGE. The arrows in A and B point to bands that disappear upon proteinase K treatment. Data shown in A and B are representative of three experiments. Molecular mass markers are shown in kDa.

equivalents for the promotion of hemopexin glycosylation by an as-yet-unidentified pathway. To determine whether the ER NADPH pool is involved, we evaluated the effect of G6-P on hemopexin glycosylation using SP cells derived from a H6PDH knockout (KO) cell line (Fig. 5A). G6-P addition still partially reversed the hypoglycosylation of hemopexin in this cell line, ruling out a role for H6PDH (Fig. 5B).

The fact that hypoglycosylation of hemopexin can be influenced by a disulfide formed via C188 led us to determine whether previously characterised PDIs that have reductase activity might be involved directly or via disulfide exchange with the STT3B subunits MagT1 or TUSC3. We focused on the PDIs ERp57 and ERdj5, as they are known to catalyse the reduction of non-native disulfides (Jessop et al., 2007; Oka et al., 2013; Ushioda et al., 2008). We created KO cell lines for the individual proteins, as well as a combined ERdj5/ERp57 double KO (Fig. 5A). For each of these cell lines there was no effect on the reversal of hypoglycosylation facilitated by G6-P (Fig. 5B). Hence, the reductive pathway maintained by the addition of G6-P functions independently of the known ER PDI reductases.

#### Role of the OST complexes containing either STT3A or STT3B catalytic subunits

To determine whether STT3A or STT3B is required for the G6-P effect on hemopexin glycosylation, we used two previously characterised KO cell lines for STT3A and STT3B (Cherepanova and Gilmore, 2016). To look specifically at glycosylation of the cysteine-proximal N187, we used the hemopexin N453Q mutant for *in vitro* translation in SP cells derived from these KO cell lines. Previously, the N453 site has been shown to be STT3B dependent (Shrimal and Gilmore, 2013). Hemopexin N453Q translated into STT3A KO SP cells was glycosylated similarly to that in wild-type cells, with both G6-P and DTT able to partially resolve the hypoglycosylation (Fig. 6A, lanes 4–6 versus lanes 1–3, and Fig. 6C). These results suggest that the effect of G6-P seen in wild-type cells is not due to the STT3A OST.

In contrast, hemopexin hypoglycosylation was more pronounced in STT3B KO cells in the absence of G6-P, with levels of 35–40% hypoglycosylation as compared with 20–25% in wild-type cells (Fig. 6B and D, compared to Fig. 6A and C). There was an effect of

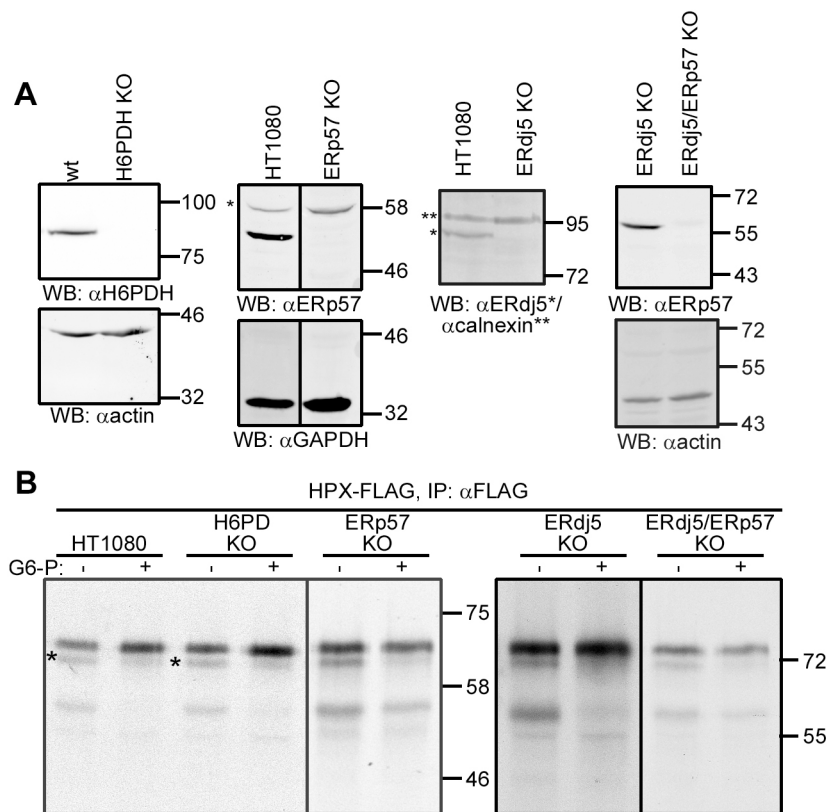


**Fig. 5. ERp57, ERdj5 or H6PDH are not required for efficient hemopexin glycosylation.** (A) Western blot (WB) analysis for H6PDH, ERp57 and ERdj5 single-KO cell lines, and for the ERp57/ERdj5 double-KO cell line, showing lack of expression for each knocked-out protein. Actin, GAPDH and calnexin are used as loading controls (wt, wild type). (B) Hemopexin (HPX-FLAG) was *in vitro* translated in the presence of SP cells derived from wild-type HT1080 cells or H6PDH, ERp57, ERdj5 or ERp57/ERdj5 KO cell lines in the absence (-) or presence (+) of 5 mM G6-P for 1 h. The *in vitro* translations were analysed as in Fig. 3. Data shown in A are representative of at least two experiments, and data in B are representative of at least three experiments. Molecular mass markers are shown in kDa.

adding G6-P or DTT, which reduced the hypoglycosylation to wild-type levels seen in the absence of reducing agent (Fig. 6D). In STT3B KO cells, not only is the STT3B catalytic activity abolished, the expression of the STT3B-specific subunits MagT1 and TUSC3 is also lost (Cherepanova and Gilmore, 2016). To see whether there is a direct contribution of MagT1 or TUSC3, we used SP cells derived from MagT1/TUSC3 double-KO cells for *in vitro* translation of hemopexin. Like with the STT3B KO cells, hemopexin hypoglycosylation was more pronounced in the absence of G6-P and, when either G6-P or DTT was included during translation, hypoglycosylation was reduced to the levels seen in wild-type cells in the absence of G6-P (Fig. 6B, lanes 4–6, and Fig. 6D). Thus, efficient glycosylation of hemopexin N187 is dependent on the STT3B complex and specifically the TUSC3 or MagT1 subunits. Importantly, the fact that there was a G6-P effect in both KO cell lines suggests that the cytosolic reductive pathway influences both STT3A- and STT3B-dependent glycosylation.

## DISCUSSION

Previous work has demonstrated a role for the STT3B-associated oxidoreductase subunits MagT1 and TUSC3 in ensuring efficient glycosylation of the STT3B-dependent substrate hemopexin (Cherepanova et al., 2014). Here, we extend this work to demonstrate that the cytosolic reductive pathway contributes towards sequon utilisation by STT3A as well as providing the optimal redox balance for STT3B activity. We find that the efficiency of cysteine-proximal acceptor site usage is dependent upon the timing of initial disulfide formation as well as post-translational reduction of disulfides by MagT1 or TUSC3 (Fig. 7). If a disulfide forms prior to glycosylation by the STT3A-containing OST, the site may be skipped and requires an STT3B-dependent reduction of the disulfide to allow glycosylation. In addition, the function of STT3B-containing OST is dependent upon the

thioredoxin-like subunits MagT1 or TUSC3, and their activity in reducing any disulfides requires a robust reductive pathway. Hence, the cytosolic reductive pathway influences the initial glycosylation by STT3A by delaying disulfide formation as well as optimising STT3B function in glycosylation of sites missed by STT3A due to rapid disulfide formation. The cytosolic reductive pathway is itself dependent upon the presence of an active pentose phosphate pathway to ensure the recycling of NADPH, illustrating a connection between cellular metabolism and glycosylation efficiency. While such a link has been suggested previously (Gansemer et al., 2020), our observations provide a previously unappreciated correlation between cellular metabolism and the variability in synthesis of protein glycoforms.

If the ability of STT3A to glycosylate the N187 sequon is determined by whether a disulfide has formed, this would indicate that the STT3B-containing OST needs to first reduce any disulfide between C188 and C200 prior to glycosylating this site. Hence, the MagT1 or TUSC3 subunits would act as reductases, which is suggested by the relatively low reduction potential of their active site thiols and by the fact that they are predominantly in an oxidised form in the ER (Cherepanova et al., 2014; Mohorko et al., 2014). In addition, substrate trapping mutants of MagT1, where the second cysteine in the C-V-V-C active site is mutated to serine, form mixed disulfides to substrate proteins, further confirming the ability to act as a reductase (Cherepanova et al., 2014). For the enzyme to function as a reductase, its active site must be reduced either by a low molecular weight thiol, such as glutathione, or by disulfide exchange with another protein. The reduction potential of glutathione is higher than that of MagT1 (Mohorko et al., 2014), so this would be a thermodynamically unfavourable reaction but cannot be ruled out due to the high cellular glutathione concentration (Jensen et al., 2009). Strong candidates for disulfide exchange reactions include members of the ER-localised PDI family, though two of the

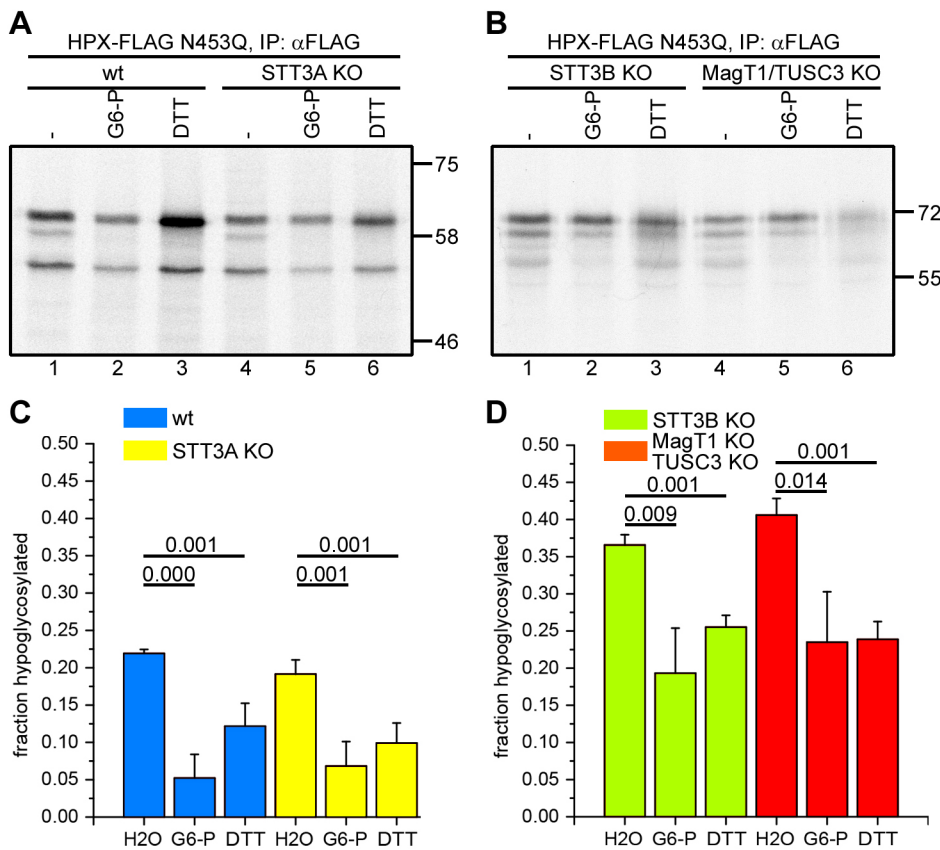


**Fig. 6. STT3A and STT3B dependence of hemopexin glycosylation.** (A,B) Hemopexin N453Q (HPX-FLAG N453Q) was translated *in vitro* in the presence of SP cells derived from (A) wild-type (wt) and STT3A KO cells, or (B) STT3B and MagT1/TUSC3 KO cells in the absence (–) or presence of 5 mM G6-P or 5 mM DTT at 30°C for 1 h. After immuno-isolation (IP), hemopexin was analysed by SDS-PAGE. Molecular mass markers in A and B are shown in kDa. (C,D) Quantification of hypoglycosylated hemopexin in (C) four independent experiments as shown in A, and (D) three independent experiments as shown in B (H<sub>2</sub>O, vehicle control). Data are presented as mean±s.d. *P*-values from Student's *t*-tests as in Fig. 1 and are shown above the bar diagrams.

previously characterised reductases, ERp57 and ERdj5, did not appear to influence the G6-P-dependent hypoglycosylation of hemopexin. Owing to the large repertoire of PDI family members (Hatahet and Ruddock, 2007), it is likely that there is redundancy in their ability to facilitate disulfide exchange, making the identification of reductases for MagT1 or TUSC3 challenging.

The transfer of reducing equivalents across the ER membrane is most likely brought about by a transmembrane protein (Cao et al., 2020), which could directly or indirectly reduce MagT1 or TUSC3.

The requirement for such a conduit for reducing equivalents has been demonstrated to allow native disulfides to form in proteins entering the secretory pathway (Poet et al., 2017). Here, the presence of such a transmembrane protein is suggested by the ability of added NADPH to partially reverse hypoglycosylation and the fact that the ER membrane is essentially non-permeant to either NADP or NADPH (Picciarella et al., 2006). This fact, combined with the lack of a role for the ER-localised H6PDH, would suggest an indirect effect on ER redox status facilitated by the transfer of reducing equivalents across the ER membrane. In addition, the ability to partially reverse hypoglycosylation using the membrane-impermeable reducing agent TCEP suggests an indirect effect on OST function. Whether the same membrane components are required to ensure the fidelity of disulfide formation and STT3B-containing OST function remains to be determined.

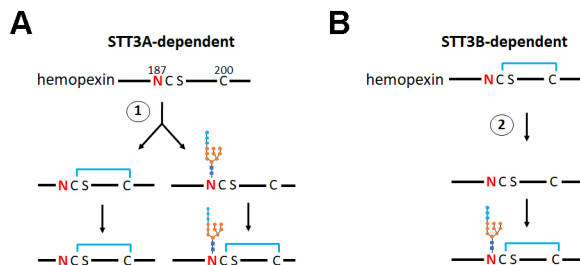


**Fig. 7. Schematic outlining the role of the cytosolic reductive pathway in determining N187 glycosylation site occupancy for STT3A- and STT3B-catalysed reactions.** During STT3A-catalysed reactions (A), glycosylation of hemopexin at N187 is dependent upon the kinetics of disulfide formation versus glycosylation at step 1. If disulfide formation occurs first (left), the site can no longer be efficiently glycosylated by STT3A. If glycosylation occurs prior to disulfide formation the latter can still form (right). Here, the reductive pathway will influence the rate of disulfide formation and therefore site occupancy. During STT3B-catalysed reactions (B) a preformed disulfide can be reduced by MagT1 or TUSC3 to allow glycosylation of N187. A lack of reduction of the disulfide prevents glycosylation of N187. The cytosolic reductive pathway contributes to the ability of MagT1 or TUSC3 to reduce the disulfide at step 2, thereby influencing glycosylation site occupancy.

## MATERIALS AND METHODS

### Cell lines, constructs and reagents

The HT1080 (CCL-121) and HEK293 (CRL-1573) cell lines were from the American Type Culture Collection (ATCC) and were cultured in DMEM (Gibco) supplemented with 2 mM glutamine, 100 U/ml penicillin, 100 µg/ml streptomycin and 10% foetal calf serum (Sigma). The STT3A, STT3B and MagT1/TUSC3 HEK 293 KO cell lines were created as described previously (Cherepanova and Gilmore, 2016). The antibodies against FLAG tag (Sigma, F3165), H6PDH (Abcam, ab119046), actin (Sigma, A2103), DNAJC10 (ERdj5) (Abnova, H00054431-M01A), calnexin (Abcam, ab22595) and GAPDH (Ambion, AM4300) were obtained commercially. The antibody to ERp57 was raised as described previously (Jessop and Bulleid, 2004). Myc- and DDK (FLAG)-tagged hemopexin plasmid was purchased from Origene. Glycosylation and cysteine mutations were made with the Quick Change II Site-Directed Mutagenesis kit (Promega). A synthetic construct coding for the hemopexin sequence without any cysteines apart from C188 was purchased from Genescript. Glucose-6-

phosphate, N-ethylmaleimide and DTT were obtained from Sigma. Tris(2-carboxyethyl) phosphine (TCEP) was purchased from Thermo Fisher Scientific.

### **In vitro transcription and in vitro translation**

Myc- and DDK (FLAG)-tagged hemopexin mRNA was transcribed from an AgeI (NEB)-linearised plasmid using T7 RNA polymerase (Promega). *In vitro* translation (Poet et al., 2017) and preparation of semi-permeabilised (SP) cells (Wilson et al., 1995) was carried out as described previously. Briefly, the mRNA was translated in a Flexi rabbit reticulocyte lysate (Promega) containing <sup>35</sup>S methionine/cysteine (Perkin Elmer) in the presence of SP cells (1 × 150,000 cells per 25 µl) at 30°C for 1 h. Where indicated, the translation reaction was supplemented with G6-P (5 mM), DTT (5 mM), TCEP (1 mM) or NADPH (1 mM). The SP cells were pelleted by centrifugation (16,162 g for 1 min) and washed with KHM buffer (110 mM KAc, 2 mM MgAc and 20 mM Hepes pH 7.2) followed by lysis [1% (v/v) Triton X-100, 50 mM Tris-HCl pH 8.0, 150 mM NaCl, 5 mM EDTA (plus a protease inhibitor tablet, Roche)], preclearing with agarose beads (Sigma, CL2B300) and immunoprecipitation with anti-FLAG antibody and protein G beads (Genscript). The samples were analysed by SDS-PAGE and visualised by exposure to film (Kodak) or phosphorimager plates (Fujifilm FLA-7000). Quantifications were performed with ImageJ (<https://imagej.nih.gov/ij/>) using phosphorimager scans and were calculated as the fraction that is hypoglycosylated [hypoglycosylated/(hypoglycosylated+fully glycosylated)].

To distinguish between translocated and non-translocated translation products, after translations the SP cells were incubated on ice with 10 µg/ml proteinase K (Roche) in the presence of 1 mM CaCl<sub>2</sub> for 25 min. The digestion was stopped with 0.5 mM PMSF before further analysis. Where indicated, the lysates were treated with endoglycosidase H (NEB).

### **CRISPR-Cas 9 KO cell lines**

Hexose-6-phosphate dehydrogenase (H6PDH) KO cells were created by CRISPR-Cas9, using a two-guide (5'-GGATTATGGAGACATGTCCT-3' and 5'-GCCATAAGTACTTCTTAGCC-3') Cas9 D10A nickase system (Kabadi et al., 2014). The same system was used for the creation of the ERp57 KO cells using the guide sequences (5'-TTCTAGCAGTCG-GAGCAG-3' and 5'-CGAGAGTCGCATCTCCGACA-3'). The ERdj5 KO cells were created using the Integrated DNA Technologies (IDT) Alt-R CRISPR-Cas 9 System; the pre-designed gRNA to knock out ERdj5 (5'-GTGTATATGGCCATTTAGT-3') was selected. We used a single gRNA (cRNA) duplexed with a tracrRNA (IDT, 1072532) and Alt-R S.p. HiFi Cas9 Nuclease V3 (IDT, 1081060) for genome editing. To generate an ERp57 KO, Cas9 nuclease was added to a duplex of 1AB crRNA:tracrRNA in Opti-MEM (Fisher, 31985062) to form the RNP complex, which was then transfected into HT1080 cells using Lipofectamine CRISPRMAX transfection reagent (Thermo Fisher Scientific). Cells were transferred to 15 cm dishes until colonies appeared (~10–12 days later). All positive KO cells were identified by western blotting using either anti-DNAJC10 (1:500 dilution) (ERdj5), anti-H6PDH (1:200 dilution) or anti-ERp57 (1:500 dilution) antibodies. For western blotting, proteins were transferred to nitrocellulose membrane (Li-Cor Biosciences), which were blocked in 3% (w/v) non-fat dried skimmed milk in TBST [Tris-buffered saline with Tween-20: 10 mM Tris, 150 mM NaCl (pH 7.5), and 0.05% (v/v) Tween-20] for 60 min. Primary antibodies were diluted in TBST, and incubations were carried out for 16 h. IRDye fluorescent secondary antibodies were used for detection, typically at 1:2500 dilutions. Blots were scanned using an Odyssey SA imaging system (Li-Cor Biosciences). Loading control antibodies were to calnexin (1:500 dilution), actin (1:250 dilution), or GAPDH (1:1000 dilution). The ERp57/ERdj5 double-KO cell line was created from the ERdj5 KO cells using the Alt-R CRISPR-Cas 9 system, with the ERp57 gRNA (5'-GTCCGTGAGTCTAGCACGT-3'; IDT).

### **Competing interests**

The authors declare no competing or financial interests.

### **Author contributions**

Conceptualization: N.J.B., M.v.L.; Methodology: M.v. L., M.A.P.; Investigation: M.v.L., M.A.P., B.F., G.G., J.I.; Resources: R.G.; Writing - original draft: N.J.B.;

Writing - review & editing: M.v.L., R.G., N.J.B.; Supervision: M.v.L., N.J.B.; Funding acquisition: N.J.B.

### **Funding**

This work was funded by the Wellcome Trust (grant number 103720) and Medical Research Scotland (grant number VAC-1417-2019). Deposited in PMC for immediate release.

### **Peer review history**

The peer review history is available online at <https://journals.biologists.com/jcs/article-lookup/doi/10.1242/jcs.259340>.

### **References**

- Allen, S., Naim, H. Y. and Bulleid, N. J. (1995). Intracellular folding of tissue-type plasminogen activator. Effects of disulfide bond formation on N-linked glycosylation and secretion. *J. Biol. Chem.* **270**, 4797-4804.
- Blomen, V. A., Majek, P., Jae, L. T., Bigenzahn, J. W., Nieuwenhuis, J., Staring, J., Sacco, R., van Diemen, F. R., Olk, N., Stukalov, A. et al. (2015). Gene essentiality and synthetic lethality in haploid human cells. *Science* **350**, 1092-1096. doi:10.1126/science.aac7557
- Blommaert, E., Peanne, R., Cherepanova, N. A., Rymen, D., Staels, F., Jaeken, J., Race, V., Keldermans, L., Souche, E., Corveleyn, A. et al. (2019). Mutations in MAGT1 lead to a glycosylation disorder with a variable phenotype. *Proc. Natl. Acad. Sci. USA* **116**, 9865-9870. doi:10.1073/pnas.1817815116
- Braunger, K., Pfeffer, S., Shrimal, S., Gilmore, R., Berninghausen, O., Mandon, E. C., Becker, T., Forster, F. and Beckmann, R. (2018). Structural basis for coupling protein transport and N-glycosylation at the mammalian endoplasmic reticulum. *Science* **360**, 215-219. doi:10.1126/science.aar7899
- Bulleid, N. J. (2012). Disulfide bond formation in the mammalian endoplasmic reticulum. *Cold Spring Harb Perspect Biol* **4**, a013219. doi:10.1101/cshperspect.a013219
- Bulleid, N. J. and van Lith, M. (2014). Redox regulation in the endoplasmic reticulum. *Biochem. Soc. Trans.* **42**, 905-908. doi:10.1042/BST20140065
- Cabibbo, A., Pagani, M., Fabbri, M., Rocchi, M., Farmery, M. R., Bulleid, N. J. and Sitia, R. (2000). ERO1-L, a human protein that favors disulfide bond formation in the endoplasmic reticulum. *J. Biol. Chem.* **275**, 4827-4833. doi:10.1074/jbc.275.7.4827
- Cao, X., Lilla, S., Cao, Z., Pringle, M. A., Oka, O. B. V., Robinson, P. J., Szmaja, T., van Lith, M., Zanivan, S. and Bulleid, N. J. (2020). The mammalian cytosolic thioredoxin reductase pathway acts via a membrane protein to reduce ER-localised proteins. *J. Cell Sci.* **133**, jcs241976. doi:10.1242/jcs.241976
- Cherepanova, N. A. and Gilmore, R. (2016). Mammalian cells lacking either the cotranslational or posttranslational oligosaccharyltransferase complex display substrate-dependent defects in asparagine linked glycosylation. *Sci. Rep.* **6**, 20946. doi:10.1038/srep20946
- Cherepanova, N. A., Shrimal, S. and Gilmore, R. (2014). Oxidoreductase activity is necessary for N-glycosylation of cysteine-proximal acceptor sites in glycoproteins. *J. Cell Biol.* **206**, 525-539. doi:10.1083/jcb.201404083
- Cherepanova, N., Shrimal, S. and Gilmore, R. (2016). N-linked glycosylation and homeostasis of the endoplasmic reticulum. *Curr. Opin. Cell Biol.* **41**, 57-65. doi:10.1016/j.cob.2016.03.021
- Cherepanova, N. A., Venev, S. V., Leszyk, J. D., Shaffer, S. A. and Gilmore, R. (2019). Quantitative glycoproteomics reveals new classes of STT3A- and STT3B-dependent N-glycosylation sites. *J. Cell Biol.* **218**, 2782-2796. doi:10.1083/jcb.201904004
- Clarke, J. L. and Mason, P. J. (2003). Murine hexose-6-phosphate dehydrogenase: a bifunctional enzyme with broad substrate specificity and 6-phosphogluconolactonase activity. *Arch. Biochem. Biophys.* **415**, 229-234. doi:10.1016/S0003-9861(03)00229-7
- Gansemer, E. R., McCommis, K. S., Martino, M., King-McAlpin, A. Q., Potthoff, M. J., Finck, B. N., Taylor, E. B. and Rutkowski, D. T. (2020). NADPH and Glutathione Redox Link TCA Cycle Activity to Endoplasmic Reticulum Homeostasis. *iScience* **23**, 101116. doi:10.1016/j.isci.2020.101116
- Hatahet, F. and Ruddock, L. W. (2007). Substrate recognition by the protein disulfide isomerases. *FEBS J.* **274**, 5223-5234. doi:10.1111/j.1742-4658.2007.06058.x
- Jensen, K. S., Hansen, R. E. and Winther, J. R. (2009). Kinetic and thermodynamic aspects of cellular thiol-disulfide redox regulation. *Antioxid Redox Signal.* **11**, 1047-1058. doi:10.1089/ars.2008.2297
- Jessop, C. E. and Bulleid, N. J. (2004). Glutathione directly reduces an oxidoreductase in the endoplasmic reticulum of mammalian cells. *J. Biol. Chem.* **279**, 55341-55347. doi:10.1074/jbc.M411409200
- Jessop, C. E., Chakravarthi, S., Garbi, N., Hammerling, G. J., Lovell, S. and Bulleid, N. J. (2007). ERp57 is essential for efficient folding of glycoproteins sharing common structural domains. *EMBO J.* **26**, 28-40. doi:10.1038/sj.emboj.7610505



- Kabadi, A. M., Ousterout, D. G., Hilton, I. B. and Gersbach, C. A.** (2014). Multiplex CRISPR/Cas9-based genome engineering from a single lentiviral vector. *Nucleic Acids Res.* **42**, e147. doi:10.1093/nar/gku749
- Kelleher, D. J., Karaoglu, D., Mandon, E. C. and Gilmore, R.** (2003). Oligosaccharyltransferase isoforms that contain different catalytic STT3 subunits have distinct enzymatic properties. *Mol. Cell* **12**, 101-111. doi:10.1016/S1097-2765(03)00243-0
- Matsuda-Lennikov, M., Biancalana, M., Zou, J., Ravell, J. C., Zheng, L., Kanellopoulou, C., Jiang, P., Notarangelo, G., Jing, H., Masutani, E. et al.** (2019). Magnesium transporter 1 (MAGT1) deficiency causes selective defects in N-linked glycosylation and expression of immune-response genes. *J. Biol. Chem.* **294**, 13638-13656. doi:10.1074/jbc.RA119.008903
- Mohorko, E., Owen, R. L., Malojcic, G., Brozzo, M. S., Aebi, M. and Glockshuber, R.** (2014). Structural basis of substrate specificity of human oligosaccharyl transferase subunit N33/Tusc3 and its role in regulating protein N-glycosylation. *Structure* **22**, 590-601. doi:10.1016/j.str.2014.02.013
- Nilsson, I. and von Heijne, G.** (2000). Glycosylation efficiency of Asn-Xaa-Thr sequons depends both on the distance from the C terminus and on the presence of a downstream transmembrane segment. *J. Biol. Chem.* **275**, 17338-17343. doi:10.1074/jbc.M002317200
- Oka, O. B., Pringle, M. A., Schopp, I. M., Braakman, I. and Bulleid, N. J.** (2013). ERdj5 is the ER reductase that catalyzes the removal of non-native disulfides and correct folding of the LDL receptor. *Mol. Cell* **50**, 793-804. doi:10.1016/j.molcel.2013.05.014
- Paoli, M., Anderson, B. F., Baker, H. M., Morgan, W. T., Smith, A. and Baker, E. N.** (1999). Crystal structure of hemopexin reveals a novel high-affinity heme site formed between two beta-propeller domains. *Nat. Struct. Biol.* **6**, 926-931. doi:10.1038/13294
- Piccirella, S., Czeglé, I., Lizak, B., Margittai, E., Senesi, S., Papp, E., Csala, M., Fulceri, R., Csermely, P., Mandl, J. et al.** (2006). Uncoupled redox systems in the lumen of the endoplasmic reticulum. Pyridine nucleotides stay reduced in an oxidative environment. *J. Biol. Chem.* **281**, 4671-4677.
- Poet, G. J., Oka, O. B., van Lith, M., Cao, Z., Robinson, P. J., Pringle, M. A., Arner, E. S. and Bulleid, N. J.** (2017). Cytosolic thioredoxin reductase 1 is required for correct disulfide formation in the ER. *EMBO J.* **36**, 693-702. doi:10.15252/embj.201695336
- Robinson, P. J. and Bulleid, N. J.** (2020). Mechanisms of disulfide bond formation in nascent polypeptides entering the secretory pathway. *Cells* **9**, 1994. doi:10.3390/cells9091994
- Roboti, P. and High, S.** (2012). The oligosaccharyltransferase subunits OST48, DAD1 and KCP2 function as ubiquitous and selective modulators of mammalian N-glycosylation. *J. Cell Sci.* **125**, 3474-3484. doi:10.1242/jcs.094599
- Ruiz-Canada, C., Kelleher, D. J. and Gilmore, R.** (2009). Cotranslational and posttranslational N-glycosylation of polypeptides by distinct mammalian OST isoforms. *Cell* **136**, 272-283. doi:10.1016/j.cell.2008.11.047
- Shibatani, T., David, L. L., McCormack, A. L., Frueh, K. and Skach, W. R.** (2005). Proteomic analysis of mammalian oligosaccharyltransferase reveals multiple subcomplexes that contain Sec61, TRAP, and two potential new subunits. *Biochemistry* **44**, 5982-5992. doi:10.1021/bi047328f
- Shrimal, S. and Gilmore, R.** (2013). Glycosylation of closely spaced acceptor sites in human glycoproteins. *J. Cell Sci.* **126**, 5513-5523. doi:10.1242/jcs.139584
- Shrimal, S., Trueman, S. F. and Gilmore, R.** (2013). Extreme C-terminal sites are posttranslocationally glycosylated by the STT3B isoform of the OST. *J. Cell Biol.* **201**, 81-95. doi:10.1083/jcb.201301031
- Ushioda, R., Hoseki, J., Araki, K., Jansen, G., Thomas, D. Y. and Nagata, K.** (2008). ERdj5 is required as a disulfide reductase for degradation of misfolded proteins in the ER. *Science* **321**, 569-572. doi:10.1126/science.1159293
- Wilson, R., Allen, A. J., Oliver, J., Brookman, J. L., High, S. and Bulleid, N. J.** (1995). The translocation, folding, assembly and redox-dependent degradation of secretory and membrane proteins in semi-permeabilized mammalian cells. *Biochem. J.* **307**, 679-687. doi:10.1042/bj3070679